Atomic Scale Electronic Characterization of Grain Boundaries in Graphene Grown by Chemical Vapor Deposition on Copper Foil

Justin C. Koepke, Joshua D. Wood, David Estrada, Eric Pop, Joseph W. Lyding

Beckman Institute, Micro and Nanotechnology Laboratory, Dept. of Electrical and Computer Engineering, Univ. of Illinois at Urbana-Champaign, 405 North Mathews Ave., Urbana, IL 61801, USA
jkoepke@illinois.edu

Wafer-scale growth of monolayer graphene is a critical step to allow integration of graphene into future nanoelectronic devices. Chemical vapor deposition (CVD) growth of graphene on copper is an area of focused research efforts due to the ability to grow predominantly monolayer graphene with the right growth conditions [1]. Recent experimental work elucidated the graphene grain boundary topology [2,3], and recent theoretical calculations simulated the electrical transport properties of ideal boundaries [4,5]. Nonetheless, to date there have been few scanning tunneling microscopy (STM) studies of graphene grown by CVD on Cu and no studies of the electronic properties of the films' grain boundaries on the atomic scale. To address this gap, we study grain boundaries in graphene grown by CVD on Cu foil using ultrahigh vacuum scanning tunneling microscopy (UHV-STM) and spectroscopy (STS).

The graphene was grown on 1.4 mil copper foil using methane in an Atomate CVD system at 1000 °C for 30 min. and transferred onto a SiO_2/n+ Si substrate after growth. Figure 1(a) shows an optical image of the graphene after the post-growth transfer to the SiO_2/Si. The dots indicate the location of the Raman spectra shown in Fig. 1(b). The G'/G ratios for these spectra suggest that the transferred graphene was indeed one monolayer. The D' band in the green spectra suggests that there was more local disorder. We degassed the sample in the UHV-STM system by direct current heating through the Si substrate at a temperature of 600–700 °C for 24 hours. Figure 1(c) shows a small STM topograph from a clean area of the sample, clearly showing the monolayer graphene lattice.

We have studied grain boundaries with misorientation angles between the grains of approximately 6°, 9°, 20°, 22°, 26°, 30°, and 32°. These grain boundaries were continuous across large protrusions and wrinkles in the graphene and other surface topography. Figure 2(a) shows the spatial derivative of an STM topograph of the meeting point of three grain boundaries. The misorientation angles between the lower-left and top grains, top and lower-right grains, and lower-left and lower-right grains approximately 9°, 22°, and 30°, respectively. Figure 2(b) shows a map of the tunneling conductance (dI/dV) recorded along the dashed green line shown in Fig. 2(a) with the color map to the right and the purple line indicating the approximate location of the grain boundary. The bottom of the dashed green line corresponds to the left side of the spectra map, and the top of the line corresponds to the right side of the spectra map. The map clearly shows larger dI/dV in empty states on the grain boundary than for spectra taken on the graphene away from the boundary. Figure 2(c) shows a comparison of the density of states (DOS), (dI/dV)/(I/V), and the dI/dV for a spectrum taken on the same grain boundary as data in Fig. 2(b) and a spectrum taken in the lower-right grain away from the boundary. These two individual specta show enhanced dI/dV in empty states and also a somewhat higher density of states in empty states at the grain boundary.

Depending on the misorientation angle between the graphene grains, we observe strong standing wave patterns adjacent to the actual grain boundaries. Figure 3(a) shows a grain boundary between two grains with a relative misorientation angle of approximately 32°. There is a clearly visible standing wave pattern on both sides of the grain boundary. Figures 3(b) and 3(c) show the fast Fourier transform (FFT) for the left and right grains, respectively, with the graphene lattice filtered out. This leaves standing waves, from which we extract their spatial extent in Fig. 3(e). Based on the misorientation angle and theory [4,5], we determine a possible grain boundary geometry, which has heptagons and pentagons as shown in Fig. 3(d). Consequently, standing waves originate from interference [6] with that particular geometry. The standing waves possess decay lengths of ~2 nm (left) and ~1.3 nm (right).

For the first time, we probe the atomic-scale electronic and topographical nature of graphene grain boundaries using STM and STS, complementing previous experimental [2,3] and theoretical work [4,5] in the field. We find that standing waves arise for scattering off particular grain boundary geometries and misorientation angles. Hence, the grain boundaries with standing waves will be deleterious for transport.

References

[1] X. Li, Science **324** (2009) 1312.
[2] P.Y. Huang, Nature AOP (2011) nature09718.
[3] J. An, arXiv: 1010.3905v1 (2010).
[4] O.V. Yazyev, Nature Materials **9** (2010) 806.
[5] O.V. Yazyev, Phys. Rev. B **81** (2010) 195420.
[6] H. Yang, Nano Letters **10** (2010) 943.

Figures

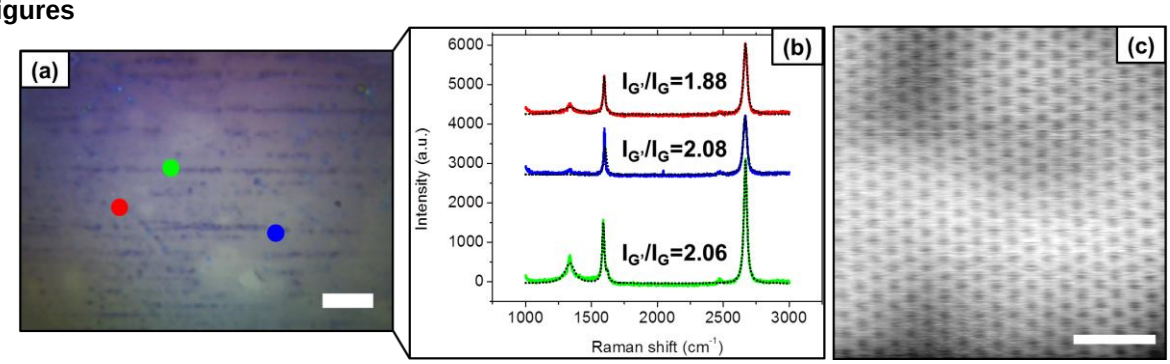

Figure 1. (a) Optical image of transferred monolayer graphene on 80 nm of SiO_2. Raman spectroscopy taken at spots indicated. Scale bar is 20 μm. (b) Raman spectroscopy of graphene, showing G', G, and D bands and Lorentzian fits in black. The green spectra has a D' band, indicating higher order disorder. All spectra have high $I_{G'}/I_G$ ratios, indicating monolayer coverage. (c) STM topograph of a clean area of the graphene. Scale bar is 1 nm.

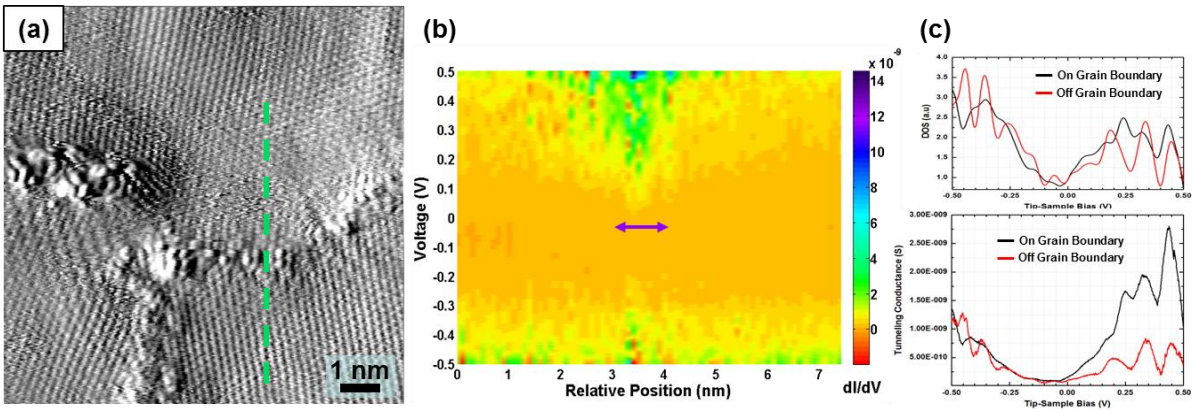

Figure 2. (a) Spatial derivative of an STM topograph of a meeting point of three grain boundaries. The misorientation angles between the graphene grains are ~22° between the top and lower-right grains, ~30° between the lower-left and lower-right grains, and ~9° between the lower-left and top grains. (b) Tunneling conductance map of calculated dI/dV spectra taken along the green dashed line from (a). The map shows a very clear enhancement of the tunneling conductance in the vicinity of the grain boundary, as indicated by the purple line on the map. (c) Comparison of tunneling conductance and normalized tunneling conductance (DOS) for a point on the grain boundary between the top and the right grains and a point away from the grain boundary in the right grain. The plots show the larger empty states dI/dV and somewhat higher empty states DOS for the spectra point on grain boundary compared to the spectra point taken away from the grain boundary.

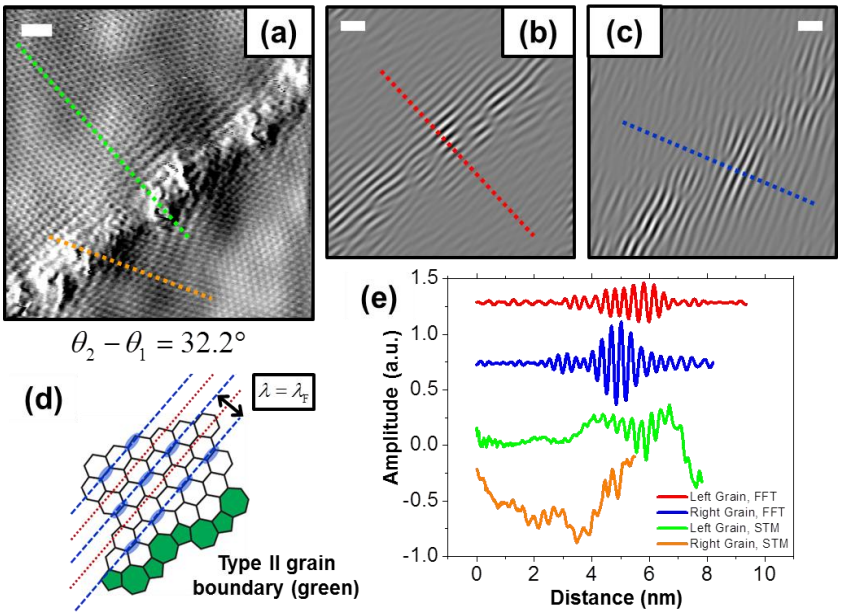

Figure 3. (a) Spatial derivative of an STM topograph of a type II grain boundary with standing waves; the misorientation angle between the two graphene lattices is ~32°. Fast Fourier transforms for the left (b) and right (c) graphene grains, with the graphene lattice filtered out, showing standing waves. (d) Schematic diagram of left graphene lattice near the heptagon-pentagon grain boundary. Light blue regions indicate interference localization along C-C bonds, giving a backscattering standing wave of wavelength λ_F (blue line, Fermi wavelength). (e) Spatial extent of standing waves, where line sections correspond to (a-c). Left grain standing wave extends ~2 nm, and right grain extends ~1.3 nm. All scale bars are 1 nm.